Research Square

Preprints are preliminary reports that have not undergone peer review.
They should not be considered conclusive, used to inform clinical practice,
or referenced by the media as validated information.

Quantification of Kinematic Characteristics Across Alpine Skiing Turn Types Using Automated Outdoor Motion Capture

Michael Zwölfer

michael.zwoelfer@uibk.ac.at

Universität Innsbruck

Giorgia Celeste Cuniberti

University of Verona and Trento

Werner Nachbauer

Universität Innsbruck

Research Article

Keywords: computer vision, recreational skiing, ski curriculum, field measurement, technique assessment

Posted Date: October 8th, 2026

DOI: https://doi.org/10.21203/rs.3.rs-10961651/v1

License: This work is licensed under a Creative Commons Attribution 4.0 International License.
Read Full License

Additional Declarations: No competing interests reported.

Quantification of Kinematic Characteristics Across Alpine Skiing Turn Types Using Automated Outdoor Motion Capture

Michael Zwölfer[1*], Giorgia Celeste Cuniberti[2,3], and Werner Nachbauer[1]

1 University of Innsbruck, Department of Sport Science, Innsbruck, Austria
2 University of Verona and Trento, CeRiSM (Research Center Sport Mountain and Health), Rovereto, Italy
3 University of Verona, Department of Neuroscience, Biomedicine and Movement Sciences, Verona, Italy
* Corresponding author: michael.zwoelfer@uibk.ac.at

Abstract

Movement descriptions in the Austrian Ski Curriculum are primarily qualitative and lack a quantitative basis across its complete range of turn types. This study therefore quantified eight standardized turn types and examined whether their kinematic characteristics evolved gradually through the curriculum. Twelve state-certified ski instructors demonstrated all techniques under real on-snow conditions. An automated eight-camera outdoor motion-capture system was used to reconstruct full-body and ski kinematics within a 250 × 80 × 30 m capture volume. Turn characteristics, center-of-mass movement, lower-limb and trunk kinematics, and ski angulation were compared using participant-level averages and linear mixed-effects models. Progression was not uniform. Prominent changes emerged at and beyond the basic-to-advanced transition: speed and lateral center-of-mass displacement increased, up-down motion showed net reductions toward the expert turns, and the center of mass shifted slightly posteriorly. Knee and hip kinematics changed from largely symmetric flexion-extension to pronounced inside-outside asymmetry, whereas ankle angles showed no systematic progression. Estimated ski edge angles increased and angles of attack decreased, particularly in carved turns. These findings provide quantitative reference data across the complete curriculum and show that the basic-to-advanced transition involves coordinated kinematic changes rather than merely faster execution of the basic turn patterns. Automated computer-vision motion capture enabled this comparison across a large outdoor sport environment.

Keywords: computer vision; recreational skiing; ski curriculum; field measurement; technique assessment

Word count: 3986; Figures: 6; Tables: 1

1 Introduction

The Austrian Ski Curriculum organizes instruction from snowplough to parallel, short, and carved turns [1]. These turn types differ in speed, radius, edging, and movement strategy, yet the curriculum defines them mainly through qualitative descriptions without an underlying quantitative characterization of the complete progression. Skiers must learn to control speed and direction while aligning the body and skis to transmit and redirect forces between the snow and the skier [2, 3]. Quantifying body and ski configurations across all standardized turn types could therefore provide an empirical reference for the mechanical demands represented at each stage.

Biomechanical studies of recreational skiing have compared selected techniques. Müller [4] examined turning techniques primarily through kinetic measures, and Debertin et al. [5] used wearable sensors to distinguish curriculum-based turn types. Full-body kinematic studies have focused mainly on alpine ski racing, where multi-camera, global navigation satellite system, and inertial approaches have quantified center-of-mass trajectories, joint motion, speed, and turn radius [6-8]. Comparisons of carved and skidded turns have also shown differences in knee loading and ski angulation [9], and video-based motion analysis has been combined with musculoskeletal simulation for a single carved turn [10]. However, no study has provided a common full-body and ski-kinematic description across the complete range of standardized recreational turn types.

Such a comparison is difficult to obtain with conventional motion-capture approaches. Marker-based optoelectronic systems provide accurate kinematics within controlled capture volumes, but many outdoor sports, like alpine skiing, require large terrain that exceeds a laboratory-sized measurement area. Manual multicamera reconstruction can be transferred outdoors but is time-consuming when many landmarks, turns, and participants are analyzed. Wearable systems cover larger fields, although they require instrumentation of the skier and do not directly reconstruct all body, ski, and pole landmarks in a shared global coordinate system. Advances in deep-learning-based keypoint detection and automated camera calibration have begun to close this gap. A previously developed and validated computer-vision system combines automated reference-point detection, skier-specific keypoint detection, frame-wise camera calibration, and multiview triangulation to reconstruct

skiing motion over large outdoor areas [11]. Applying that system to the complete curriculum provides an opportunity to move from technical validation to a substantive biomechanical use case.

The primary purpose of this study was to provide a quantitative description of turn characteristics, center-of-mass (COM) movement, lower-limb and trunk kinematics, and ski angulation across all turn types defined in the Austrian Ski Curriculum. A secondary purpose was to examine whether and how these kinematic components evolved between successive turn types. We hypothesized that higher-level turn types would show higher speed, larger radius, shorter duration, greater lateral COM displacement, reduced up-down COM motion, a more posterior COM position, larger estimated edge angles, and smaller angles of attack. Based on the curriculum progression, we expected these characteristics to change gradually across the eight techniques rather than to be dominated by a single transition.

2 Methods

2.1 Participants

Twelve state-certified Austrian ski instructors (age, 25 ± 4 y; height, 171 ± 5 cm; mass, 68 ± 5 kg) participated. All participants were free from injury and experienced in demonstrating the curriculum turn types. The study was approved by the Board for Ethical Questions in Science of the University of Innsbruck (certificate 35/2021; 17 May 2021) and was conducted in accordance with the Declaration of Helsinki. All participants received information about the procedures and provided written informed consent.

2.2 Field test and procedure

Field testing was conducted on a ski slope in Zürs am Arlberg, Austria. The capture volume measured approximately 250 × 80 × 30 m and contained nearly 300 surveyed reference points arranged in two corridors. Corridor 1 had a mean inclination of 19 degrees and was used for advanced parallel long (APL), carving long (CL), advanced parallel short (APS), and expert short (ES) turns. Corridor 2 had a mean inclination of 12 degrees and was used for snowplough (SP), snowplough to parallel (SPP), basic parallel long (BPL), and basic parallel short (BPS) turns. Testing was performed on grippy natural snow. After each measurement block, the slope was side-slipped to restore comparable surface conditions.

Eight consumer-grade camcorders (Sony AX53, Tokyo, Japan) were positioned around the capture volume and recorded at 3840 × 2160 pixels and 25 Hz. The cameras were panned, tilted, and zoomed to maintain sufficient skier image size. Each reference point consisted of a wooden pole with a 9 × 9 × 9 cm cube carrying ArUco markers on all sides. Reference-point coordinates were surveyed with a Trimble S3 total station (Trimble Inc, Westminster, Colorado). Ski equipment was standardized: all participants used Head e-Speed skis with a nominal sidecut radius of 19 m and lengths of 175 cm for women and 185 cm for men. Ski boots were individual.

After a short warm-up, each participant completed one run of each turn type. The turn types and their curriculum definitions are provided in Table 1. Runs were performed in four measurement blocks and in the following order: APL in Corridor 1 and SP in Corridor 2; CL in Corridor 1 and SPP in Corridor 2; APS in Corridor 1 and BPL in Corridor 2; and ES in Corridor 1 and BPS in Corridor 2. All cameras recorded simultaneously. A run was included only when at least four cameras recorded the complete run successfully. Recordings were synchronized by dropping a foam cube with ArUco markers along a vertical rod at the beginning and end of each capture session [11]. All 12 participants attempted all eight turn types (96 planned runs). Twenty-six runs were excluded because fewer than four cameras recorded the complete run successfully, leaving 70 runs for analysis.

Table 1 Turn types according to the Austrian Ski Curriculum [1]

Name	Abbrev.	Characteristics	Level
Snowplough	SP	The entire turn is performed in a snowplough position; the inside edges control speed and direction.	Basic
Snowplough to parallel	SPP	Direction change begins in a snowplough position; after the fall line, the turn is completed with the skis parallel.	Basic
Basic parallel long	BPL	The entire turn is performed with the skis parallel and skidded at moderate speed through long-radius turns.	Basic
Basic parallel short	BPS	The entire turn is performed with the skis parallel and skidded at moderate speed through short-radius turns.	Basic
Advanced parallel long	APL	The turn is performed with the skis parallel and skidded at higher speed through long-radius turns.	Advanced

Name	Abbrev.	Characteristics	Level
Advanced parallel short	APS	The turn is performed with the skis parallel and skidded at higher speed through rhythmic short turns.	Advanced
Carving long	CL	The turn is performed with the skis parallel and carved at high speed through long arcs.	Expert
Expert short	ES	The turn is performed with the skis parallel and skidded at high speed through rhythmic short turns.	Expert

Note. Definitions were adapted from the Austrian Ski Curriculum [1]

2.3 Automated outdoor motion capture

The complete procedures for synchronization, reference-point detection, skier-specific keypoint detection, calibration, reconstruction, and validation are reported elsewhere [11]. The workflow relevant to the present application is summarized in Fig. 1. Reference cubes were localized automatically using a YOLO object detector [12] trained on more than 20,000 annotated cube images and identified with the OpenCV ArUco module [13]. Temporal matching maintained reference identities when individual markers were briefly blurred or occluded.

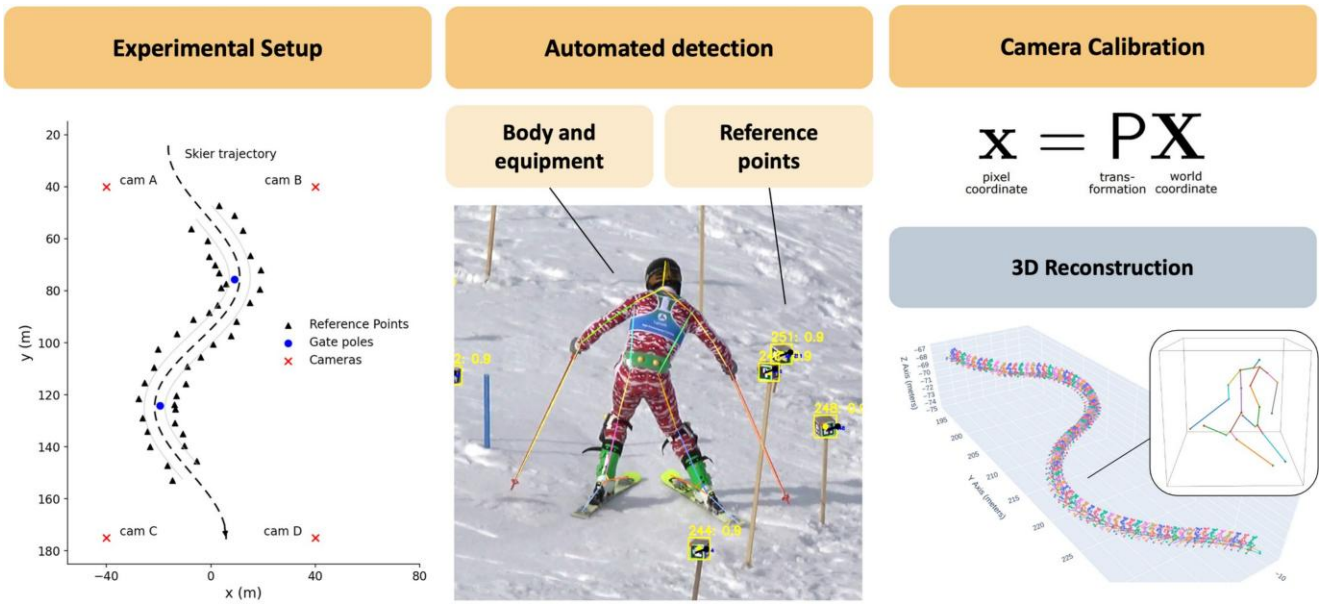


Fig. 1 Methodological workflow. Left: schematic representation of the field setup; corridor geometry is simplified and not to scale. Middle: example camera view showing detected reference cubes and skier-specific keypoints. Right: camera calibration and three-dimensional reconstruction used to derive biomechanical trajectories and metrics. The workflow figure was created for the present manuscript based on the procedures described in [11]

Skier and equipment landmarks were detected by fine-tuning the pretrained HALPE26 AlphaPose model [14] to predict a skier-specific set of 24 keypoints. The output comprised the head and neck; bilateral shoulders, elbows, wrists, pole baskets, hips, knees, and ankles; and bilateral front and rear binding locations, ski tips, and ski tails. Training used more than 10,000 manually annotated skiing images from the field test and previous studies. The sport-specific output allowed the skier's body and equipment to be reconstructed within the same coordinate system.

Frame-wise camera projection matrices were calculated by direct linear transformation from the automatically detected reference points and their surveyed three-dimensional coordinates [15]. The 15 reference points closest to the skier were selected in each frame, and iterative outlier rejection removed unreliable correspondences. Keypoints detected in at least four camera views were triangulated using singular value decomposition. A consistent set of cameras was used within each run to support temporal stability. The resulting trajectories were filtered with a fourth-order low-pass Butterworth filter with a cutoff frequency of 10 Hz.

2.4 Biomechanical variables

The COM was estimated from the reconstructed body keypoints using a segmental model with anthropometric mass fractions [16]. COM speed was calculated as the time derivative of its trajectory. Turn radius was estimated by fitting circles to a sliding window of COM positions, and turn duration was defined as the time between successive turn transitions.

A skier-based coordinate system described COM position relative to the skis. The longitudinal axis extended from the mean ski-tail position to the mean ski-tip position. The up-down axis was normal to the plane formed by the ski longitudinal axis and the vector between the feet, and the lateral axis completed the orthogonal system. The vector from the mean foot-support point to the COM was projected onto these axes to calculate lateral, up-down, and fore-aft COM position.

Ankle, knee, and hip angles were calculated as three-point angles in three dimensions and reported separately for the inside and outside leg. Trunk inclination was calculated between the shoulder-hip vector and the up-down axis. Ski edge angle was estimated as the complementary angle between the shank vector and the snow-surface normal. Angle of attack was calculated between the ski longitudinal axis and the instantaneous COM velocity vector.

2.5 Turn segmentation and statistical analysis

For parallel turns, turn onset was defined as the instant at which lateral COM displacement crossed zero. For SP and SPP, onset was defined by maximum up-down COM position because lateral displacement remained close to zero. Trajectories were time-normalized from 0% to 100% of the turn cycle. Maximum, minimum, and mean values were extracted. Mean turn radius was calculated from 30% to 80% of the turn cycle to avoid the near-infinite radii around the transition [17]. For each participant and turn type, values from all valid turns in a single run were averaged before statistical analysis. Final analyzed-participant and valid-turn counts for each technique are reported in the supplementary material (Online Resource 1). Participant-level means were compared across turn types using linear mixed-effects models with turn type as a fixed effect and participant as a random intercept. Omnibus F statistics, p values, and partial eta-squared effect sizes were calculated using Satterthwaite's approximation for degrees of freedom. Pairwise contrasts of estimated marginal means used Tukey adjustment for multiple comparisons. Central contrasts are reported as mean differences with 95% confidence intervals. Statistical significance was set at $p = .05$. Analyses were conducted in MATLAB R2024b (MathWorks, Natick, MA, USA) and R (R Foundation for Statistical Computing, Vienna, Austria) using RStudio 2025.05 (Posit Software, PBC, Boston, MA, USA).

3 Results

3.1 Turn characteristics

Turn characteristics differed mainly between the basic and higher-level turn types (Fig. 2). Mean speed showed a significant main effect of turn type ($F(7, 46.0) = 292.92$, $p < .001$, partial $\eta^2 = 0.98$). Speed increased modestly from SP through SPP to BPL and then increased from BPL to APL (mean difference = 7.36 m/s, 95% CI [5.89, 8.82], $p < .001$) and from APL to CL (mean difference = 2.68 m/s, 95% CI [1.23, 4.12], $p < .001$), reaching approximately 15 m/s in CL. In short turns, speed increased from BPS to APS (mean difference = 3.84 m/s, 95% CI [2.82, 4.86], $p < .001$) and remained similar in ES ($p = .581$).

Mean radius also varied across techniques ($F(7, 32.3) = 35.36$, $p < .001$, partial $\eta^2 = 0.88$), ranging from 7.7 m in BPS to 19 m in CL. Long-turn radius increased from BPL to APL (mean difference = 9.84 m, 95% CI [5.07, 14.60], $p < .001$), whereas APS and ES had similar radii ($p = .997$).

Turn duration showed a significant main effect of turn type ($F(7, 41.2) = 284.49$, $p < .001$, partial $\eta^2 = 0.98$). Long-turn duration decreased from approximately 4 s in the basic turns to 1.9 s in CL. The reduction from BPL to APL was significant (mean difference = -1.39 s, 95% CI [-1.86, -0.91], $p < .001$), whereas the further decrease from APL to CL was not significant after Tukey adjustment ($p = .199$). Short-turn duration decreased from 1.5 s in BPS to approximately 0.7 s in APS and ES, driven by a reduction from BPS to APS (mean difference = -0.67 s, 95% CI [-1.22, -0.12], $p = .008$); APS and ES durations did not differ ($p = 1.000$). At the advanced and expert levels, long turns were faster, had larger radii, and had longer durations than the corresponding short turns (all $p < .001$).

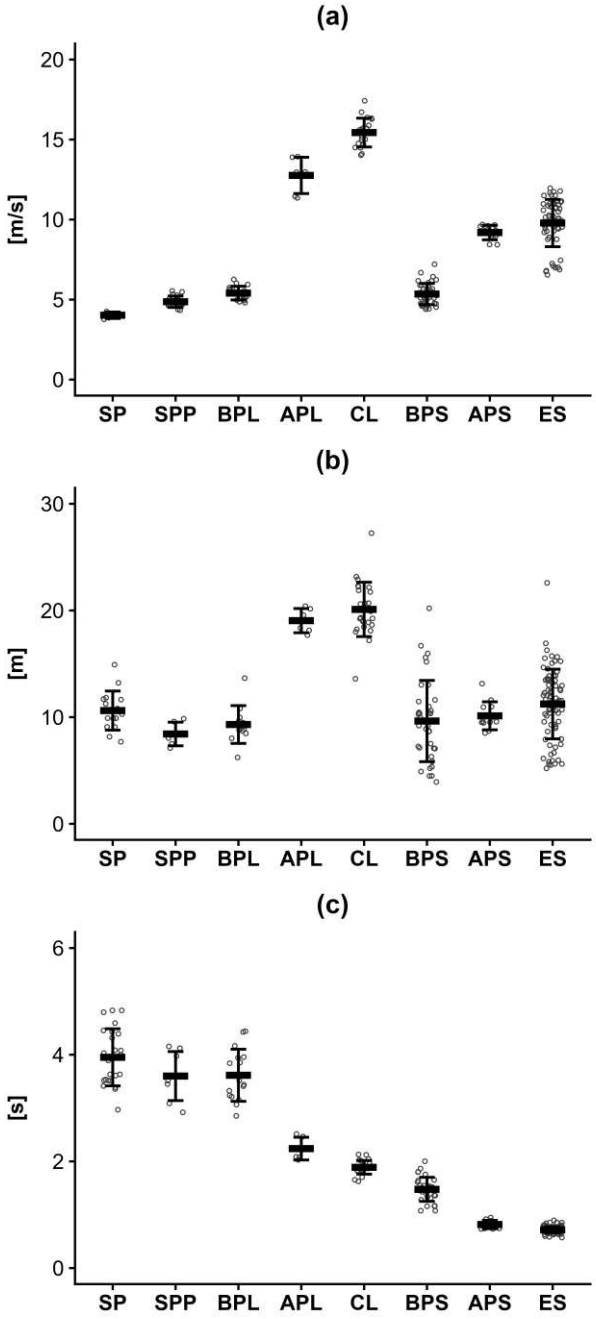


Fig. 2 Distributions of speed (a), turn radius (b), and turn duration (c) across all turn types. Open circles represent individual valid turns, and horizontal bars indicate mean ± standard deviation (SD). Inferential analyses used participant-level averages

3.2 Center-of-mass movement

COM movement showed a pronounced change across turn types (Figs. 3 and 4). Maximum lateral displacement differed across turn types ($F(7, 38.9) = 39.22$, $p < .001$, partial $\eta^2 = 0.88$), increasing from 0.16 m in SP to 0.59 m in CL and from 0.34 m in BPS to 0.44 m in ES. The increase from BPL to APL was significant (mean difference = 0.15 m, 95% CI [0.04, 0.26], $p = .002$). The increase from BPS to APS did not reach significance after Tukey adjustment ($p = .155$), whereas the net increase from BPS to ES was significant (mean difference = 0.10 m, 95% CI [0.02, 0.18], $p = .003$). Long turns showed a broad lateral-displacement plateau through the central part of the cycle, whereas short turns showed a rounded trajectory.

Peak up-down COM values also showed a main effect of turn type ($F(7, 35.4) = 14.90$, $p < .001$, partial $\eta^2 = 0.75$). Up-down COM motion tended to decrease across the curriculum. The direct steps from BPL to APL ($p = .974$) and from BPS to APS ($p = .144$) were not significant, whereas net reductions were evident from BPL to CL (mean difference = -0.08 m, 95% CI [-0.13, -0.03], $p < .001$) and from BPS to ES (mean difference = -0.10 m, 95% CI [-0.15, -0.05], $p < .001$).

Fore-aft COM position varied among techniques ($F(7, 46.0) = 33.96$, $p < .001$, partial $\eta^2 = 0.84$). The COM shifted posteriorly from BPL to CL (mean difference = -0.16 m, 95% CI [-0.23, -0.09], $p < .001$) and from BPS to ES (mean difference = -0.25 m, 95% CI [-0.32, -0.18], $p < .001$), while the overall fore-aft range decreased.

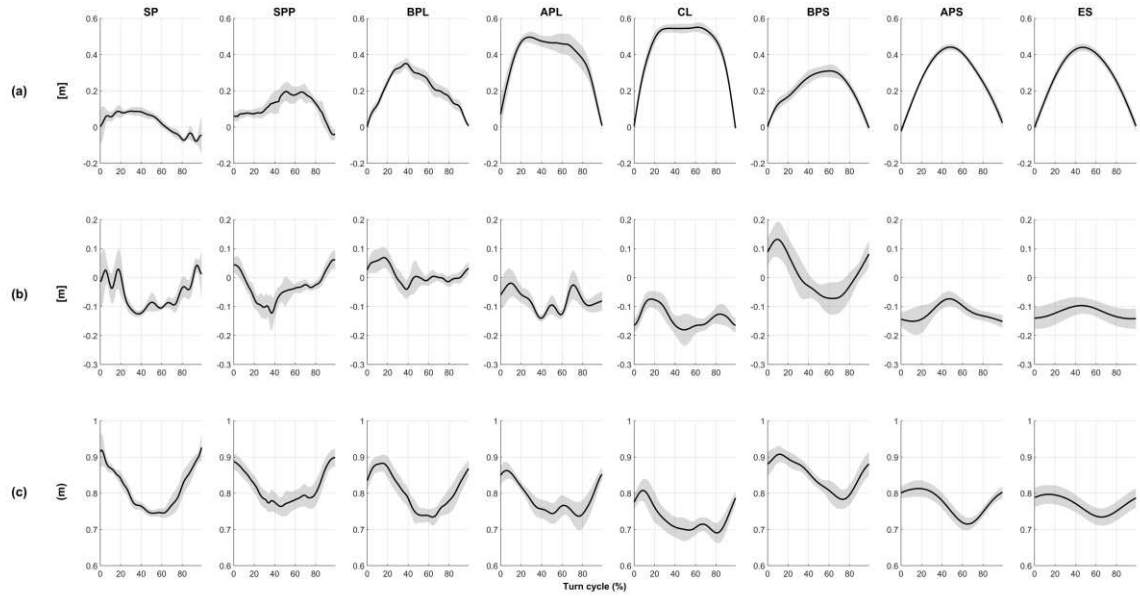


Fig. 3 Center-of-mass trajectories for lateral (a), fore-aft (b), and up-down (c) position across all turn types. Curves show mean ± SD and are time-normalized to one complete turn cycle

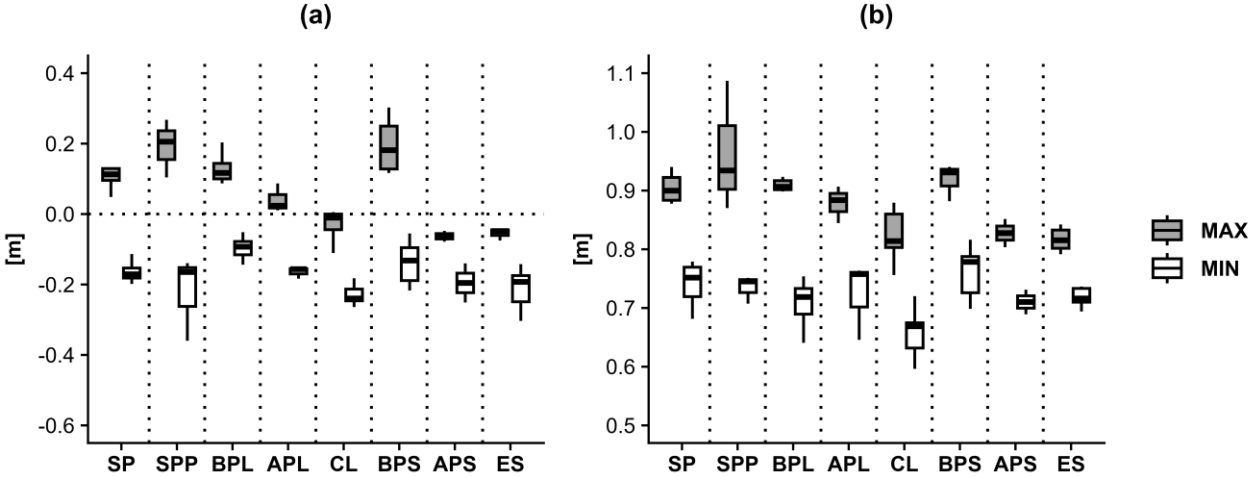


Fig. 4 Maximum and minimum center-of-mass positions in the fore-aft (a) and up-down (b) directions across turn types. Box-and-whisker plots show participant-level values

3.3 Lower-limb and trunk kinematics

Lower-limb coordination changed from largely symmetric to asymmetric patterns (Fig. 5). Ankle angles remained between approximately 70° and 85° and showed no clear systematic progression across turn types. In SP, SPP, BPL, and BPS, the inside- and outside-knee trajectories were largely parallel. Knee kinematics showed main effects of turn type for both the inside ($F(7, 34.5) = 21.80$, $p < .001$, partial $\eta^2 = 0.82$) and outside leg ($F(7, 36.4) = 4.34$, $p = .001$, partial $\eta^2 = 0.46$). In APL and CL, the outside knee remained more extended, while the inside knee flexed more. From BPL to CL, maximum inside-knee flexion increased (mean difference = -22.68°, 95% CI [-33.16°, -12.19°], $p < .001$), dropping below 90° in CL, whereas

the outside knee showed no significant change (mean difference = -4.67°, 95% CI [-14.79°, 5.46°], p = .812). This divergence produced an inside-outside difference of approximately 30° near mid-turn. A similar but smaller asymmetry appeared from BPS to APS and remained in ES.

Hip angles showed the same general change, with main effects for both the inside ($F(7, 27.4) = 31.52$, $p < .001$, partial $\eta^2 = 0.89$) and outside hip ($F(7, 33.6) = 7.89$, $p < .001$, partial $\eta^2 = 0.62$). The inside hip flexed markedly in APL and CL, whereas the outside hip remained more extended. Trunk inclination also showed a main effect of turn type ($F(7, 39.8) = 16.06$, $p < .001$, partial $\eta^2 = 0.74$). Trunk inclination shifted toward larger angles with increasing turn level, while its range of motion narrowed.

3.4 Ski angulation

Ski angulation reflected the transition from snowplough to parallel and carved turns (Fig. 6). Maximum estimated edge angles showed main effects of turn type for both the outside ski ($F(7, 38.3) = 129.13$, $p < .001$, partial $\eta^2 = 0.96$) and inside ski ($F(7, 46.0) = 66.15$, $p < .001$, partial $\eta^2 = 0.91$). SP showed opposing and asymmetric edging, with maximum estimated edge angles of approximately 35° for the outside ski and 25° for the inside ski. SPP became more symmetric after the fall line, and BPL showed similar estimated edge angles for both skis. Edge angles increased from BPL to APL for both the outside ski (mean difference = 20.79°, 95% CI [13.69°, 27.88°], $p < .001$) and inside ski (mean difference = 12.63°, 95% CI [4.31°, 20.94°], $p < .001$). The increase continued from APL to CL for the outside ski (mean difference = 11.09°, 95% CI [4.15°, 18.04°], $p < .001$) and inside ski (mean difference = 10.15°, 95% CI [1.96°, 18.33°], p = .006), reaching approximately 66° for the outside ski and 58° for the inside ski in CL. In short turns, estimated edge angle increased from BPS to APS for the outside ski (mean difference = 19.50°, 95% CI [11.06°, 27.94°], $p < .001$) and inside ski (mean difference = 13.56°, 95% CI [3.71°, 23.40°], p = .002). Edge angles then remained similar in ES (both p = 1.000).

Angles of attack were asymmetric in SP and SPP, became similar between the skis in BPL, and showed a main effect across the parallel turn types ($F(5, 31.9) = 3.24$, p = .018). The angle of attack decreased to approximately 10° in CL and was lower than in APL (mean difference = -1.89°, 95% CI [-3.53°, -0.26°], p = .016). No clear differences in angle of attack occurred among the short turns (BPS to APS: p = .999; APS to ES: p = 1.000).

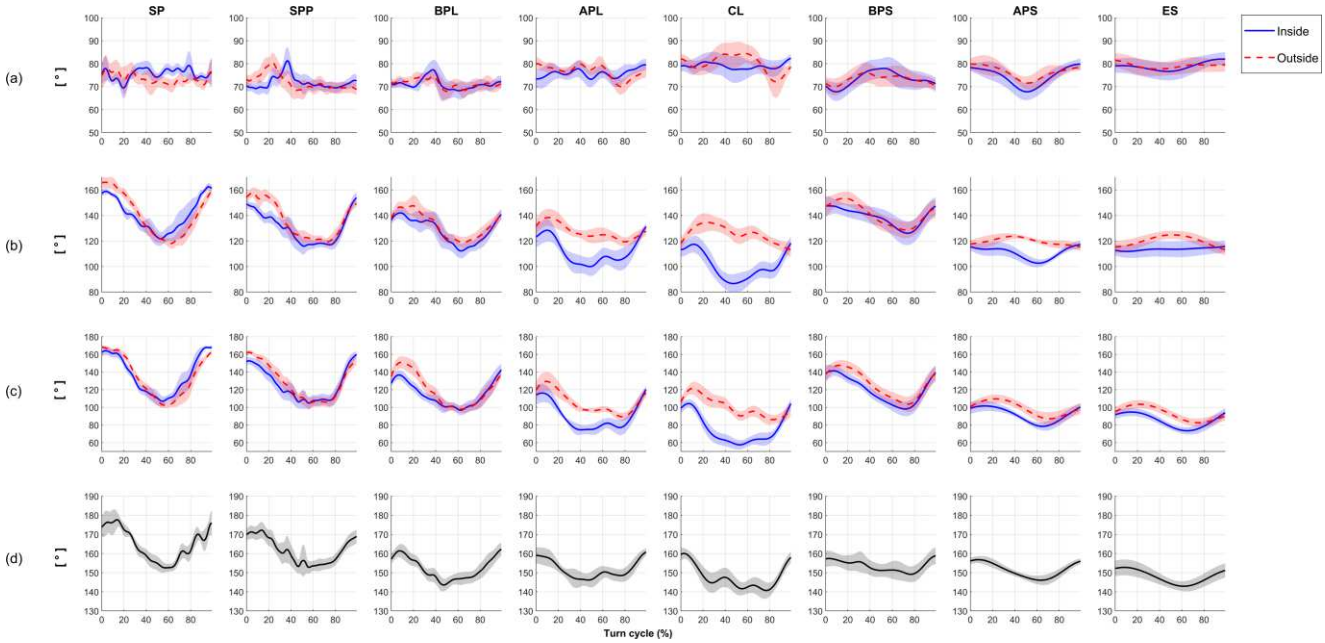


Fig. 5 Ankle (a), knee (b), hip (c), and trunk-inclination (d) trajectories across all turn types. Curves show mean ± SD and are time-normalized to one complete turn cycle. Inside-leg angles are shown as blue solid lines, outside-leg angles as red dashed lines, and trunk inclination as a black solid line

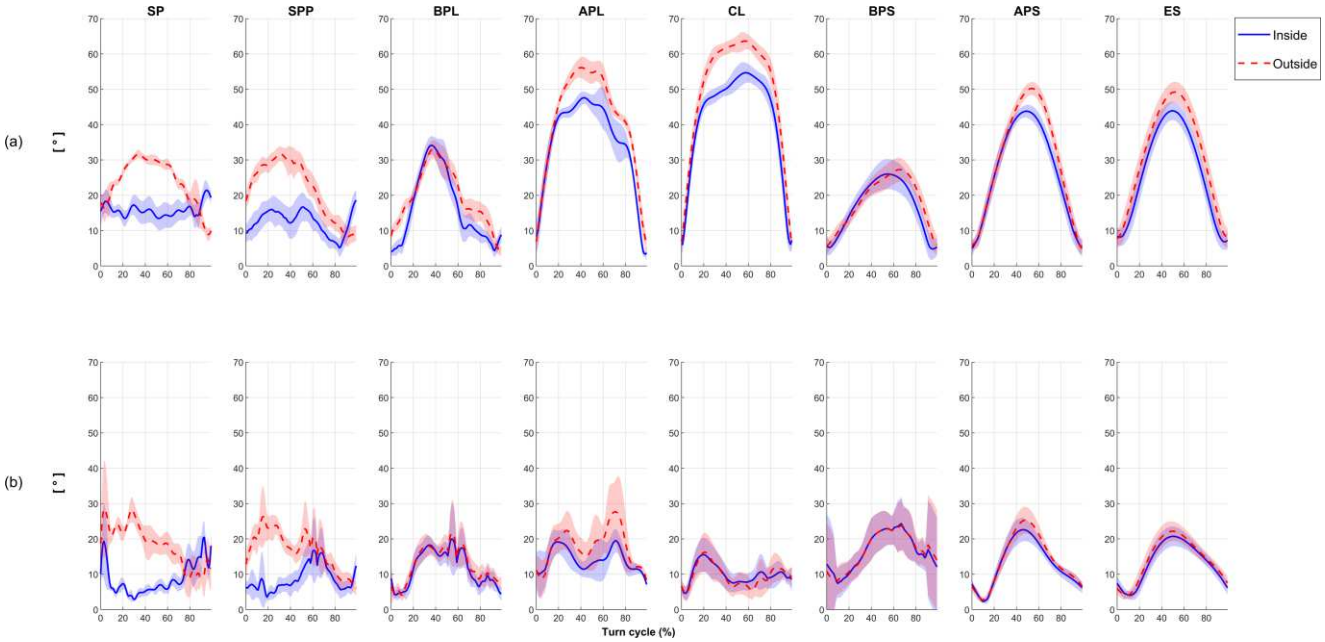


Fig. 6 Estimated ski edge-angle (a) and angle-of-attack (b) trajectories across all turn types. Curves show mean ± SD and are time-normalized to one complete turn cycle. Inside-ski angles are shown as blue solid lines and outside-ski angles as red dashed lines

4 Discussion

This study provided a quantitative description of turn characteristics, COM movement, joint kinematics, and ski angulation across all turn types defined in the Austrian Ski Curriculum. When the changes between successive techniques were examined, the expected gradual progression was not observed. Instead, several coordinated changes emerged at the basic-to-advanced transition and continued into the expert turns: speed and lateral COM displacement increased, net up-down COM motion decreased toward the expert turns, the COM shifted slightly posteriorly, knee and hip kinematics became strongly asymmetric, and estimated edge angles increased. Ankle motion showed no systematic progression. Because the same state-certified instructors demonstrated all techniques, the results describe standardized curriculum turn types rather than movement patterns of skiers with different abilities or learning over time.

The speed, radius, and duration results characterize the task conditions under which the standardized turns were demonstrated. The largest changes from BPL to APL and from BPS to APS coincided with the transition to steeper terrain and faster execution. CL speed was slightly higher than reported in a previous comparison of recreational carved and skidded turns [9], while CL radius was comparable with values reported for giant-slalom turns [6, 18]. The radii and durations of the short turns were close to values reported for slalom skiing [18, 19]. These comparisons do not make the curriculum turns equivalent to racing turns, but they show that advanced demonstrations approached mechanical conditions investigated previously in competitive skiing.

The COM trajectories show how whole-body positioning changed under these conditions. Greater lateral displacement in APL, CL, APS, and ES was consistent with the larger estimated edge angles and the need to balance over an inclined support. The broad plateau in the long turns indicates that this position was maintained through much of the steering phase, whereas the rounded profile in short turns reflects the shorter time available before the next transition. Up-down COM motion tended to decrease at the basic-to-advanced transition, although the direct pairwise changes were not significant; significant net reductions emerged from basic to expert turns. At higher speed, rapid redirection of the resultant reaction force during edge change may reduce the need for pronounced active movement along the up-down axis. The more posterior COM position may partly result from greater knee and hip flexion combined with restricted ankle movement in the ski boot [20, 21]. It should not automatically be interpreted as an ineffective backseat position. However, the present kinematic data cannot determine the exact position or direction of the resultant force.

The joint-angle trajectories further indicate a change in coordination strategy. At the basic level, both legs flexed and extended in a largely synchronous manner. In APL and CL, the outside leg remained more extended while the inside knee and hip flexed markedly. This configuration may facilitate lateral displacement and edging while allowing the outside leg to support a greater share of the load. Similar inside-outside asymmetries have been reported in giant-slalom and carved turns

[6, 9]. Trunk motion also became less variable while mean inclination increased, consistent with the trunk acting as a comparatively stable link while the legs control inclination and ski angulation.

The ski-angulation trajectories connected these body changes to the technical definitions of the turn types. SP and the first part of SPP showed the asymmetric ski positions created by the snowplough. BPL was the first technique with parallel and symmetric edging. Estimated edge angles then increased sharply in APL and CL and in APS relative to BPS. The values in CL were close to edge angles reported in giant-slalom skiing [6, 19], although the present measure was derived from shank orientation. Angles of attack remained relatively high in the skidded turns and decreased only in CL, consistent with the distinction between skidded and carved execution [9]. ES retained a larger angle of attack than CL because it remained a skidded technique despite its expert classification.

Taken together, the results show that progression was not entirely gradual. The concentration of changes at the basic-to-advanced transition suggests a coordinated kinematic reorganization, especially in task speed, lateral COM control, lower-limb coordination, and ski angulation. This pattern is not explicitly reflected in the current Austrian Ski Curriculum, which differentiates APL from BPL primarily through higher speed and associated task demands [1]. The present data indicate that APL was not simply a faster BPL demonstration; it also involved changes in lateral COM displacement, leg coordination, and edge angle. This does not establish a single causal mechanism, but it identifies a coherent change in the movement solution used to perform the prescribed turns. For ski instruction, the values provide quantitative references for standardized demonstrations. They should not be treated as fixed thresholds that every learner must reproduce, because individual technique will depend on anthropometry, equipment, terrain, snow, speed, and the instructional task.

The automated workflow generated sport-specific three-dimensional trajectories of the skier and equipment across a large outdoor field [11]. Beyond enabling the present comparison, this type of scalable data generation may provide a basis for developing skier-specific single-view three-dimensional pose-estimation methods. Synchronized multiview images paired with reconstructed three-dimensional keypoints can support the training and evaluation of models that infer skier and ski motion from a single, uncalibrated camera. Such approaches could extend quantitative analysis to training or injury videos for which calibrated multiview recordings are unavailable. The trajectories and reference values may also support automated turn classification and technique assessment, provided that task and terrain context are considered rather than evaluating technique from kinematics alone.

Several limitations should be considered. The turn types were performed on two slopes because the curriculum prescribes different terrain and speed conditions; slope inclination, speed, radius, and technique therefore changed together and their individual effects cannot be separated. Expert demonstrations may not reproduce the variability or errors of learners. Each participant completed one run per technique, and data availability depended on complete multiview coverage. Snow spray and other occlusions could reduce keypoint visibility, while calibration accuracy depended on stable detection of the surveyed reference points. The study measured kinematics but not ski-snow forces, plantar pressure, or joint loading. Edge angle was estimated from shank orientation rather than measured directly from the ski, and the 24-keypoint model supported flexion-extension analysis but not full three-dimensional joint rotations. Finally, the different onset definition for SP and SPP may have introduced small phase shifts relative to the parallel turns.

5 Conclusions

Kinematic characteristics across the eight standardized alpine skiing turn types did not follow a uniform gradual progression. The most prominent coordinated changes emerged at the basic-to-advanced transition and continued toward the expert turns: faster execution coincided with greater lateral COM displacement, net reductions in up-down motion, a slightly more posterior COM position, pronounced inside-outside knee and hip asymmetry, and larger estimated ski edge angles. Automated outdoor motion capture made this full-body and equipment-level comparison possible over a large on-snow capture volume. The resulting data provide quantitative references across the complete curriculum and a basis for future computer-vision systems for turn classification and feedback.

Acknowledgements

We gratefully acknowledge Daniel Huber and the Ski Club Arlberg for providing the slope, resources, and slope preparation. We thank Katja Wolfram, Maximilian Lamprecht, and Christopher Krabath for their support during the field study, as well as the students of the biomechanics seminar for their assistance.

References

1. Österreichischer Skischulverband (2018) Snowsport Austria: Die österreichische Skischule. Österreichischer Skischulverband, Innsbruck
2. Howe J (2001) The new skiing mechanics, 2nd edn. McIntire Publishing, Waterford
3. LeMaster R (2010) Ultimate skiing. Human Kinetics, Champaign
4. Müller E (1994) Analysis of the biomechanical characteristics of different swinging techniques in alpine skiing. J Sports Sci 12:261-278. https://doi.org/10.1080/02640419408732172
5. Debertin D, Wachholz F, Mikut R, Federolf P (2022) Quantitative downhill skiing technique analysis according to ski instruction curricula: a proof-of-concept study applying principal component analysis on wearable sensor data. Front Bioeng Biotechnol 10:1003619. https://doi.org/10.3389/fbioe.2022.1003619
6. Spörri J, Kröll J, Schwameder H, Müller E (2012) Turn characteristics of a top world class athlete in giant slalom: a case study assessing current performance prediction concepts. Int J Sports Sci Coach 7:647-659. https://doi.org/10.1260/1747-9541.7.4.647
7. Gilgien M, Crivelli P, Spörri J, Kröll J, Müller E (2015) Characterization of course and terrain and their effect on skier speed in World Cup alpine ski racing. PLoS One 10:e0118119. https://doi.org/10.1371/journal.pone.0118119
8. Fasel B, Spörri J, Gilgien M, Boffi G, Chardonnens J, Müller E, Aminian K (2016) Three-dimensional body and centre of mass kinematics in alpine ski racing using differential GNSS and inertial sensors. Remote Sens 8:671. https://doi.org/10.3390/rs8080671
9. Klous M, Müller E, Schwameder H (2012) Three-dimensional knee joint loading in alpine skiing: a comparison between a carved and a skidded turn. J Appl Biomech 28:655-664. https://doi.org/10.1123/jab.28.6.655
10. Heinrich D, van den Bogert AJ, Mössner M, Nachbauer W (2023) Model-based estimation of muscle and ACL forces during turning maneuvers in alpine skiing. Sci Rep 13:9026. https://doi.org/10.1038/s41598-023-35775-4
11. Zwölfer M, Mössner M, Rhodin H, Nachbauer W (2026) Outdoor motion capture at scale. Sensors 26:1951. https://doi.org/10.3390/s26061951
12. Ultralytics (2023) YOLOv8: advanced real-time object detection system. https://docs.ultralytics.com. Accessed 14 July 2026
13. Bradski G (2000) The OpenCV library. Dr Dobb's J Softw Tools 25:120-123
14. Fang HS, Li J, Tang H et al (2023) AlphaPose: whole-body regional multi-person pose estimation and tracking in real-time. IEEE Trans Pattern Anal Mach Intell 45:7157-7173. https://doi.org/10.1109/TPAMI.2022.3222784
15. Abdel-Aziz YI, Karara HM (1971) Direct linear transformation from comparator coordinates into object space coordinates in close-range photogrammetry. In: Proceedings of the symposium on close-range photogrammetry. American Society of Photogrammetry, pp 1-18
16. de Leva P (1996) Adjustments to Zatsiorsky-Seluyanov's segment inertia parameters. J Biomech 29:1223-1230. https://doi.org/10.1016/0021-9290(95)00178-6
17. Zorko M, Nemec B, Babič J, Lešnik B, Supej M (2015) The waist width of skis influences the kinematics of the knee joint in alpine skiing. J Sports Sci Med 14:606-619
18. Supej M, Holmberg HC (2010) How gate setup and turn radii influence energy dissipation in slalom ski racing. J Appl Biomech 26:454-464. https://doi.org/10.1123/jab.26.4.454
19. Kröll J, Spörri J, Kandler C, Fasel B, Müller E, Schwameder H (2015) Kinetic and kinematic comparison of alpine ski racing disciplines as a base for specific conditioning regimes. ISBS Proc Arch 33:1401-1404
20. Hsiao ET (1994) A dynamic model to study the influence of alpine ski boot characteristics on heel retention force. Master's thesis, Rochester Institute of Technology
21. Shealy JE, Miller DA (1987) Dorsiflexion of the human ankle as it relates to ski boot design in downhill skiing. Proc Hum Factors Soc Annu Meet 31:1128-1132. https://doi.org/10.1177/154193128703101012

Statements and Declarations

Funding

The authors declare that no funds, grants, or other support were received during the preparation of this manuscript.

Competing interests

The authors have no relevant financial or non-financial interests to disclose.

Author contributions

Michael Zwölfer: conceptualization, methodology, software, validation, investigation, data curation, visualization, writing - original draft, and writing - review and editing. Giorgia Celeste Cuniberti: methodology, statistical analysis, visualization,

and writing - review and editing. Werner Nachbauer: conceptualization, resources, project administration, and supervision. All authors approved the submitted version and agree to be accountable for the work.

Data availability

The datasets and code used for data processing, keypoint-detection fine-tuning, three-dimensional reconstruction, and statistical analysis are available from the authors upon reasonable request.

Ethics approval

The study was approved by the Board for Ethical Questions in Science of the University of Innsbruck (certificate 35/2021; 17 May 2021) and conducted in accordance with the Declaration of Helsinki.

Consent to participate

All participants received information about the procedures and provided written informed consent.

Supplementary Files

This is a list of supplementary files associated with this preprint. Click to download.

- SupplementaryMaterialSportsEngineering.pdf